Low-frequency limit for H/V studies due to tilt
Tilt induced acceleration versus inertial acceleration

Thomas Forbriger
BFO (Schiltach) and GPI (Karlsruhe)
October 2006

1 Low-frequency H/V peak

Throughout the data recorded during the URS project (Ritter et al., 2005) in Bucharest city Ziehm (2006) observes a low-frequency peak in H/V ratio near 0.2 Hz. The frequency of this peak is systematically varying from lower frequencies in the north to higher frequencies in the south. This variation presumably is caused by the dipping of the interface between the cretaceous and the neogene with depth varying from 1000 m to 2000 m (Mândrescu et al., 2004). Unfortunately in the recordings of most stations the H/V level strongly rises with frequency decreasing below 0.15 Hz. This puts an effective limit on the analysis of the peak at frequencies below 0.2 Hz (Fig. 1). Since in some of the data there appears to be a power-law relation between H/V ratio and frequency below 0.15 Hz, I discuss tilt as a possible cause of this strong increase.

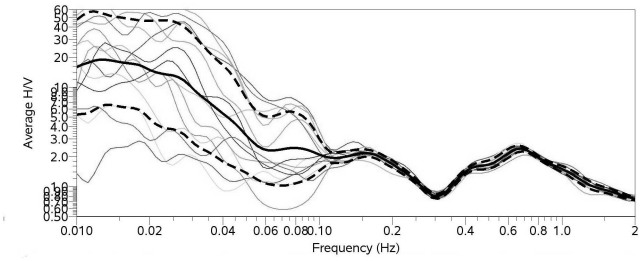

Figure 1: H/V ratio calculated from the data of station URS 14 obtained during the URS experiment in Bucharest city. Time windows in the range from June 22nd 2004 21:00 UTC to June 23rd 2:00 UTC were used. Each gray curve displays the H/V ratio for one time window, while the black curve gives the average and the dashed curves mark the standard deviation. Two peaks are observed. One at 0.15 Hz, the other at 0.7 Hz. For frequencies below 0.15 Hz peaks may be obscured by the increasing and unstable values of H/V ratio. Courtesy of Julia Ziehm.

2 Forces acting on an inertial sensor

Gravimeter, seismometers and tiltmeters all use a mass as physical sensor. They sense inertial and gravitational acceleration and are principally unable to distinguish between both sources of forces acting on them (Wielandt, 2002, secs. 2.1 and 3.3).

Consider a displacement field $\vec{u}(\vec{x},t)$. I distinguish the vertical component $u_z(h,z,t)$ and the horizontal component $u_h(h,z,t)$, where z is the vertical coordinate (positive in upward direction), h is the horizontal coordinate, and t is time. From this follows the inertial acceleration in the horizontal direction

$$a_h = \frac{\partial^2 u_h}{\partial t^2} \tag{1}$$

and

$$a_z = \frac{\partial^2 u_z}{\partial t^2} \tag{2}$$

in vertical direction. Assuming that the sensor sits on the floor it additionally senses an acceleration due to the component of gravity $\vec{g} = -g\hat{e}_z$ (with $\hat{e}_z$ pointing upward) that is coupled into its sensitive direction due to ground tilt. For small tilt angles the contribution to the vertical component ist negligible, while it can be significant for the forces sensed by the horizontal components (Wielandt and Forbriger, 1999). For small tilt angles the resulting acceleration signal acting on the horizontal component of the seismometer may be approximated by

$$a_\tau = g\frac{\partial u_z}{\partial h}. \tag{3}$$

If $\tilde{a}_z$, $\tilde{a}_h$, and $\tilde{a}_\tau$ are the Fourier transforms of a_z, a_h, and a_τ, respectively, the Fourier transform of the seismometer's vertical component output signal is

$$\tilde{s}_z(\omega) = T(\omega)\tilde{a}_z(\omega), \tag{4}$$

where $T(\omega)$ is the instrument's complex response function. And

$$\tilde{s}_h(\omega) = T(\omega)\left(\tilde{a}_h(\omega) + \tilde{a}_\tau(\omega)\right), \tag{5}$$

is the Fourier transform of the seismometer's horizontal component output signal.

3 Tilt contribution to H/V ratio

H/V ratio is calculated from seismic recordings usually by

$$A_{\mathrm{H/V}}(\omega) = \frac{|R(\omega)\tilde{s}_h(\omega)|}{|R(\omega)\tilde{s}_z(\omega)|} = \frac{|\tilde{a}_h(\omega) + \tilde{a}_\tau(\omega)|}{|\tilde{a}_z(\omega)|} \tag{6}$$

and averaging over signals from several time windows. $R(\omega)$ is the response function of a deconvolution filter that provides a displacement signal from the electrical output signal $s(t)$. Hence the H/V ratio contains a tilt contribution, which may be ignored at high frequencies since the inertial effect rises with ω^2. At low frequencies the tilt contribution is likely to dominate $A_{\mathrm{H/V}}$.

4 Point load on an elastic halfspace

The elastic deformation of a homogeneous halfspace due to a static point load is known as the „Boussinesque solution“ in the theory of elasticity. According to Zürn (2003) the solution to Boussinesque's problem is

$$u_z(r,z) = -\frac{F}{4\pi\mu}\frac{1}{R}\left(\frac{\lambda+2\mu}{\lambda+\mu}+\frac{z^2}{R^2}\right) \tag{7}$$

for the vertical component and

$$u_r(r,z) = -\frac{F}{4\pi(\lambda+\mu)}\frac{1}{r}\left(1+\frac{z}{R}+\frac{\lambda+\mu}{\mu}\frac{r^2 z}{R^3}\right) \tag{8}$$

for the horizontal component in cylindrical coordinates with $r=\sqrt{x^2+y^2}$ being the radial coordinate, $R=\sqrt{r^2+z^2}$ being the spacial distance to the load, the loading force at the origin being

$$\vec{f} = -F\delta(\vec{x})\hat{e}_z \tag{9}$$

and λ and μ being Lamés parameters for the homogeneous halfspace at $z<0$.

For observations at the surface of the elastic halfspace

$$u_z(r,z=0) = -\frac{F}{4\pi\mu}\frac{1}{r}\frac{\lambda+2\mu}{\lambda+\mu} \tag{10}$$

for the vertical component and

$$u_r(r,z=0) = -\frac{F}{4\pi(\lambda+\mu)}\frac{1}{r} \tag{11}$$

for the horizontal component, which is valid for $r>0$.

If $F(t)$ varies with time but so slowly that the deformation instantaneously follows the variation of the load and elastic wave contribution to the displacement field is negligible, this is the seismic near field. In this case the accelerations acting on the seismometer are

$$a_z(t,r,z=0) = -\frac{\ddot{F}(t)}{r}\frac{\lambda+2\mu}{4\pi\mu(\lambda+\mu)}, \tag{12}$$

$$a_h(t,r,z=0) = -\frac{\ddot{F}(t)}{r}\frac{1}{4\pi(\lambda+\mu)}, \tag{13}$$

and

$$a_\tau(t,r,z=0) = g\frac{\partial u_z(t,r,z)}{\partial r} \tag{14}$$

$$= g\frac{F(t)}{r^2}\frac{\lambda+2\mu}{4\pi\mu(\lambda+\mu)}. \tag{15}$$

For the corresponding Fourier transforms of the seismometer's output signals I obtain

$$\tilde{s}_z(\omega) = T(\omega)\tilde{F}(\omega)\frac{1}{4\pi(\lambda+\mu)}\frac{\omega^2}{r}\frac{\lambda+2\mu}{\mu} \tag{16}$$

and

$$\tilde{s}_r(\omega) = T(\omega)\tilde{F}(\omega)\frac{1}{4\pi(\lambda+\mu)}\left(\frac{\omega^2}{r}+\frac{g}{r^2}\frac{\lambda+2\mu}{\mu}\right), \tag{17}$$

where $\tilde{F}(\omega)$ is the Fourier transform of the point load's time history $F(t)$. This results in

$$A_{\mathrm{HIV}}(\omega) = \frac{\frac{\omega^2}{r}+\frac{g}{r^2}\frac{\lambda+2\mu}{\mu}}{\frac{\omega^2}{r}\frac{\lambda+2\mu}{\mu}} \tag{18}$$

$$= \frac{\mu}{\lambda+2\mu}+\frac{g}{r\omega^2}. \tag{19}$$

The high-frequency limit is

$$\lim_{\omega\to\infty} A_{\mathrm{HIV}}(\omega) = \frac{\mu}{\lambda+2\mu} \tag{20}$$

and the low-frequency limit is

$$\lim_{\omega\to 0} A_{\mathrm{HIV}}(\omega) = \frac{g}{r\omega^2} \tag{21}$$

and rises with $1/\omega^2$ for decreasing frequency ω. Both contributions are equal at

$$\omega_C = \sqrt{\frac{g}{r}\frac{\lambda+2\mu}{\mu}}. \tag{22}$$

Consider a point load at $r=10\,\mathrm{m}$ distance, with $\lambda=\mu$ in the halfspace and $g=9.81\,\mathrm{m\,s^{-2}}$. Then

$$\omega_C = 2\pi\cdot 0.27\frac{1}{\mathrm{s}}. \tag{23}$$

The H/V ratio will become $A_{\mathrm{HIV}}>2$ at frequencies $f<0.11\,\mathrm{Hz}$ due to the tilt contribution, which is then likely to mask the ellipticity of surface waves. Additional examples are displayed in Fig. 2.

5 Propagating surface wave

The displacement field of the harmonic component ω of plane surface waves is given by

$$u_z(r,t) = A(\omega)\sin(k(\omega)r-\omega t) \tag{24}$$

and

$$u_r(r,t) = A(\omega)\,\varepsilon(\omega)\cos(k(\omega)r-\omega t), \tag{25}$$

where $A(\omega)$ is a frequency dependent amplitude, $\varepsilon(\omega)$ is the frequency dependent ellipticity, and $k(\omega)$ is the frequency dependent wavenumber. For prograde waves

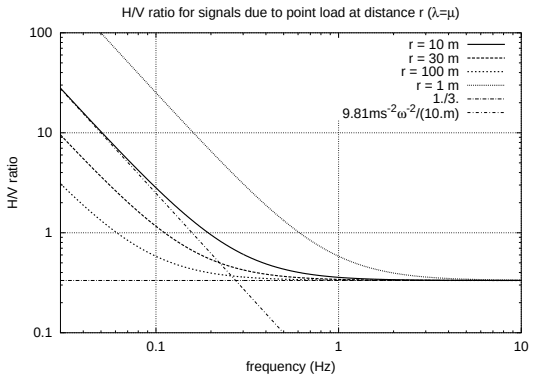

Figure 2: H/V ratio predicted by eq. (19) for a point load at various distances r. Lamé's constants are assumed to be equal ($\lambda = \mu$).

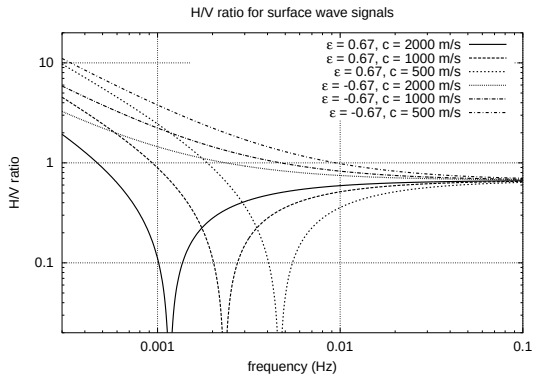

Figure 3: H/V ratio predicted by eq. (30) for surface waves of constant phase velocity c and constant ellipticity ε.

$\varepsilon < 0$ and $\varepsilon > 0$ for retrograde waves. For the accelerations acting on the seismometer I obtain

$$a_z(r,t) = -\omega^2 A(\omega)\,\sin(k(\omega)r - \omega t), \tag{26}$$

$$a_r(r,t) = -\omega^2 A(\omega)\,\varepsilon(\omega)\,\cos(k(\omega)r - \omega t), \tag{27}$$

and

$$a_\tau(r,t) = gk(\omega)A(\omega)\,\cos(k(\omega)r - \omega t). \tag{28}$$

For the H/V ratio this immediately results in

$$A_{\mathrm{HIV}}(\omega) = \frac{\left|gk(\omega) - \omega^2\varepsilon(\omega)\right|}{\omega^2} \tag{29}$$

$$= \left|\frac{g}{\omega c(\omega)} - \varepsilon(\omega)\right|, \tag{30}$$

where $c(\omega) = \omega/k(\omega)$ is the phase velocity.

Assuming $\varepsilon(\omega)$ and $c(\omega)$ are bounded, the high-frequency limit provides the ellipticity.

$$\lim_{\omega\to\infty} A_{\mathrm{HIV}}(\omega) = \varepsilon(\omega) \tag{31}$$

and the low-frequency limit is

$$\lim_{\omega\to 0} A_{\mathrm{HIV}}(\omega) = \frac{g}{\omega c(\omega)}. \tag{32}$$

Both cancel at

$$\omega_C = \frac{g}{\varepsilon c} \tag{33}$$

for retrograde waves. For prograde waves they are equal at ω_C.

Consider a surface wave with $c = 2000\,\mathrm{m\,s^{-1}}$, $\varepsilon = 0.67$, and $g = 9.81\,\mathrm{m\,s^{-2}}$. Then

$$\omega_C = 2\pi \cdot 1.2 \cdot 10^{-3}\frac{1}{\mathrm{s}}. \tag{34}$$

Additional examples are displayed in Fig. 3.

6 Conclusions

Generally we assume to observe the ellipticity of surface waves, when studying H/V ratio. Additionally to microseisms propagating as surface waves, we have to expect point load varying with time (moving vehicles, buildings loaded by wind, etc.) close to the seismic instruments in an urban environment. In this case we have to expect a combination of effects described by eqs. (19) and (30) in the H/V ratio.

It is however not correct to simply add the results for A_{HIV} caused be different sources. To estimate the H/V ratio individual contributions of surfaces waves, point loads and other sources must first be added in the numerator and denominator of eq. (6) prior to taking the ratio. The relative strength of the point load compared to the surface wave amplitude thus controls whether the point load effect can take over the H/V ratio at low frequencies or not. This may explain the strong scatter of H/V from different time windows at frequencies below 0.1 Hz in Fig. 1. For the same reason we will never be able to observe the cancellation of the contributions to the horizontal component acceleration in eq. (29), neither as a hole in H/V nor as a peak in V/H. Horizontal acceleration due to other sources introduce a waterlevel in the total horizontal acceleration.

Typical peaks in H/V ratio that are commonly attributed to Rayleigh wave ellipticity range between values of 2 and 10. In the high-frequency range the peaks caused by Rayleigh wave ellipticity will dominate in any case. However, at low-frequencies tilt contribution to the horizontal signal can dominate the H/V ratio. The effect for tilt due to surface waves may become significant at frequencies below 10 mHz, which is outside

the bandwidth studied with the URS data. The effect of tilt induced by point loads at a distance of 10 m, however, can dominate the H/V ratio and can explain the observations made with URS data.

7 Acknowledgements

I'm grateful to Julia Ziehm for providing Fig. 1 and to Walter Zürn and Olivier Sèbe for inspiring discussions. URS data was recorded with the KABBA arrays within the framework of CRC 461.

References

Mândrescu N., Radulian M. and Mărmureanu G., 2004. Site conditions and predominant period of seismic motion in the Bucharest urban area. Rev. Roum. Géophysique, 48: 37–48.

Ritter J.R.R., Balan S., Bonjer K.P., Diehl T., Forbriger T., Mărmureanu G., Wenzel F. and Wirth W., 2005. Broadband urban seismology in the bucharest metropolitan area. Seism. Res. Lett., 76(5): 574–580.

Wielandt E., 2002. Seismic sensors and their calibration. In: P. Bormann and E. Bergmann (editors), *New Manual of Seismological Observatory Practice*, GeoForschungsZentrum, Potsdam, Germany. <http://www.geophys.uni-stuttgart.de/seismometry/man_html/index.html>, <http://www.geophys.uni-stuttgart.de/downloads/Postscript-files>.

Wielandt E. and Forbriger T., 1999. Near-field seismic displacement and tilt associated with the explosive activity of Stromboli. Annali di Geofisica, 42(3): 407–416. <http://www-gpi.physik.uni-karlsruhe.de/pub/forbriger/>.

Ziehm J., 2006. Seismisches Monitoring einer Großstadt, Analyse von H/V Spektralverhältnissen. Diplomarbeit, Geophysikalisches Institut, Universität Karlsruhe. in preparation.

Zürn W., 2003. Boussinesque-problem: Point load on an elastic halfspace. A compilation of 12 published solutions to Boussinesque's problem. Unpublished manuscript.